UNIVERSITÀ DI PISA

**DIPARTIMENTO DI INGEGNERIA DELL'ENERGIA DEI SISTEMI DEL TERRITORIO E DELLE COSTRUZIONI**

**RELAZIONE PER IL CONSEGUIMENTO DELLA LAUREA MAGISTRALE IN INGEGNERIA GESTIONALE**

# *CAD surface modeling from freeform, branched and incomplete point clouds*

## SINTESI

---

RELATORI

Prof. Ing. Michele Lanzetta
*Università di Pisa, Dipartimento di Ingegneria Civile e Industriale*

Prof. Monique Chyba
*University of Hawai'i at Mānoa, Department of Mathematics*

Dr. Sonia Rowley
*University of Hawai'i at Mānoa, Department of Earth Science*

IL CANDIDATO

Francesco Lupi

Sessione di Laurea Magistrale del 29/04/2020
Consultazione NON consentita
Anno accademico 2018/2019

# Sommario

La ricostruzione CAD di superfici a partire da nuvole di punti complesse tramite elaborazione automatica è un problema aperto in letteratura, specialmente nel caso di grandi moli di dati. In aggiunta alla numerosità dei dati, la disposizione libera nello spazio 3D, l'incompletezza, il rumore, la disuniformità e le sezioni variabili delle nuvole di punti in input sono le principali variabili caratterizzanti la complessità sopracitata. Riuscire a gestire così tante variabili contemporaneamente potrebbe avere un enorme impatto sulla possibilità di digitalizzare oggetti naturali o artefatti quali prodotti o impianti industriali. La presente tesi è stata svolta presso UH Mānoa e ha avuto come input un esempio di nuvola di punti contraddistinta dalle caratteristiche sovraesposte, risultato di un problema di fotogrammetria applicata a delle immagini di un corallo. Sono stati quindi sviluppati quattro differenti metodi per ricostruzione CAD di superfici da nuvole di punti complesse e sono stati comparati proponendo un nuovo scenario di valutazione quantitativa della qualità degli stessi. Ogni metodo, che offre differenti vincoli sulle nuvole di punti in input, differenti qualità delle mesh in output e differente costo, deve essere scelto in base alle applicazioni specifiche.



# Abstract

CAD surface reconstruction from complex point clouds through an automatic data processing has not yet been solved in the literature, especially when dealing with big clouds. Adding to that, the 3D freedom layout, incompleteness, noisy, not uniformity and variable radius section of the input data are the main variables linked to the complexity above mentioned. Handle all these variables together would have a tremendous impact for the digitalization of natural or human artifacts as industrial systems or products. This thesis has been carried out at UH Manoa and examines the case of a point cloud characterized by the above features, result of a close-range photogrammetry problem applied to a coral's photos. Then, four different methods for CAD surface reconstruction have been developed and compared proposing new quantitative assessment framework on the quality of them. Each mesh generator, that offers a different degree of constraints on the input point cloud, output mesh quality and cost, must be chosen based on the target application.

# 1 Introduction

Since the advent of the Computer Aided Design era, a lot of work has been carried out on 3D digitalization of objects. In particular, the 3D modeling of points cloud is a huge issue remains unsolved when dealing with noisy, freeform and incomplete data [8]. Applications of the previous topic span from industrial scenario (e.g. reverse engineering [9] and chemical pipe systems digitalization [10], [11], [12], [13]) to medicine [14], architecture [15], design [16], archeology [17], [18] and biology [19] fields of research. The main issue is to synthetize the information of the 3D real-world subjects onto a digital-twin replica as much close to the original one. Below three examples of laser scanned point clouds coming from different contexts.

**Figure 1**: *Piping system [10].*

**Figure 2**: *Artifact [24].*

**Figure 3**: *Building [15].*

## 1.1 Problem

The context of this study is a multidisciplinary project focused on Pohnpei[1] exploration, called '*Pohnpei 360°: Aerial to the Mesophotic'*, in collaboration with the departments of Earth Sciences, Mathematics, and Biology at the University of Hawai'i at Mānoa. The problem arose during the researches dealing with a unique coral in the mesophotic coral ecosystem, the Gorgonian Sea Fan. After preprocessing some close-range underwater pictures and development ad-hoc solutions integrated to standard structure-from-motion photogrammetry software tools [5], a 3D point cloud has been extracted. Due the extreme complexity of the subject is not feasible to go further using the same software [5], or others well known software as [36], to convert the point cloud to a final mesh.

## 1.2 Scope and Goal

This work has been carried out in order to solve a practical problem related to the 3D modeling of a complex point cloud that currently commercial software can't solve. The definition of complexity here is related to 5 aspects: free 3D layout, incompleteness, noisy, not uniformity and variable section. The goal is to develop a technique as more

[1] Federals states of Micronesia

general as possible, that deal with such as complex point clouds, no matter if coming from a laser scanner or a photogrammetric approach, with the only constraints about the pseudo-circular section. The 3D model's texture and color appearance are out of scope but could be an interesting additional topic for future works.

**Figure 4:** *Gorgonian sea fan point cloud, extracted by Sfm software [5]. Total points: 389777.*

# 2 State of the art and related works

Geometrical models generated from a point clouds captured from a real object has an infinite current type of application and huge relevance in several industries [20]. The main related works to recall are "*The power crust"* [20], "*Fast Cylinder Shape Matching using RANSAC*" [21] and "*Efficient and robust reconstruction of botanical branching structure from laser scanned points*" [19]. The first one generates mesh and approximates medial axis using as references sampled points of the original 3D point cloud [20]. The second one is a technique implemented for pipe meshing problems, based on cylinders approximation by spheres [21]. The latter is an extremely interesting study that deal with freeform branched structure offering a modeling approach based on tree's laser scanned points cloud [19]. The issue is that state of the art techniques and commercial software deal with pretty good input point clouds, mainly laser scanner data. For inaccurate and raw point clouds coming from photogrammetry much work can be done and several questions are still answered. For example, cause the complexity of such point clouds, is

not possible to use classical triangles meshing techniques based on connectivity to the input data as in [22], [23]. The presented approach is a simple theory but not trivial implementation to solve a practical problem otherwise not solvable. Meshing cylindrical surfaces using the 3D skeleton information as discussed by [20], [21], [19], [11] is the building block of this study. Pursuing this idea, the methods 1, 2 and 3 respectively in *Section 3.3, 3.4* and *3.5* extract the 3D skeleton using a well-known algorithm that deal with a complex point cloud, "*L-1 Medial Skeleton"* [24]. Other 3D skeleton remarkable techniques and applications discussed in [25], [26], [27]. This is the main advantage of the methods presented in this study compared to the researches in [20], [21], [11], [19]. The key strength of L-1 Medial Skeleton is that "*it does not place strong requirements on the quality of the input point cloud nor on the geometry or topology of the captured shape and it can be directly applied to an unoriented raw point scan with significant noise, outliers, and large areas of missing data"* [24].

# 3 Methods

Four surface reconstruction algorithms have been developed on the same point cloud fitting the above mentioned complexity characteristics, the gorgonian point cloud, *(Fig.4).*

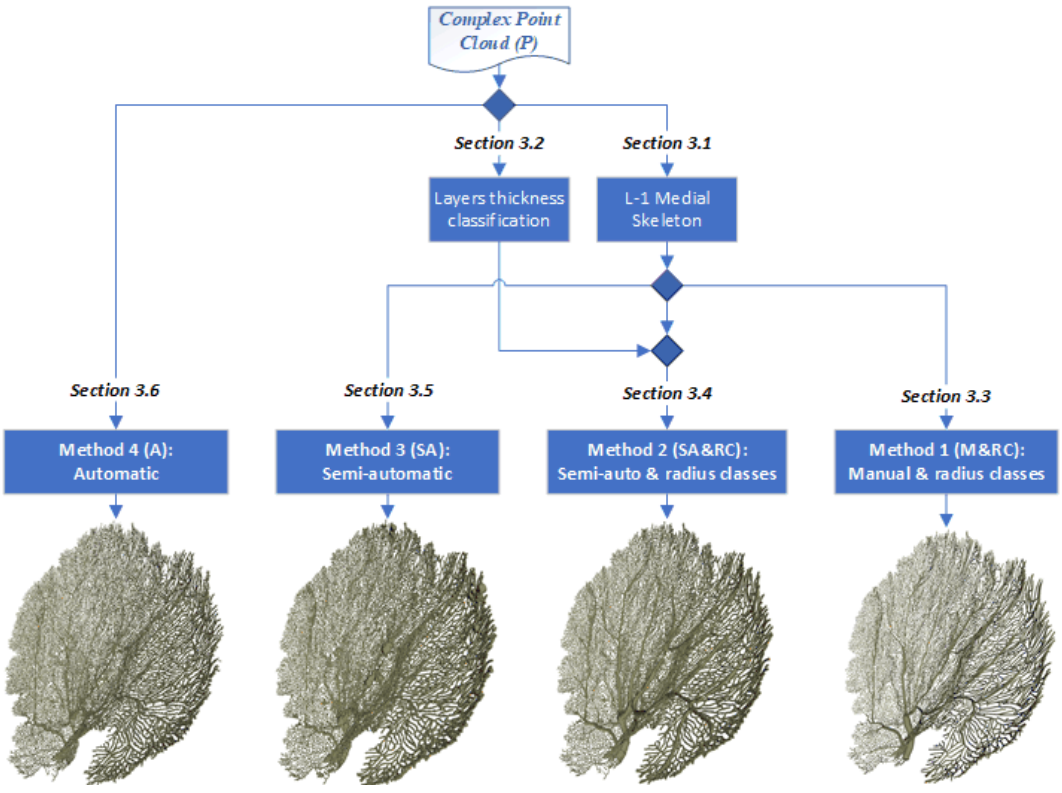


**Figure 5:** *Methods flow chart and output meshes.*

## 3.1 Skeleton points extraction from point cloud data

The complexity of the point cloud $\boldsymbol{P}$ = $\{points \in Gorgonian\ point\ cloud\}$ cause difficulty to evaluate the 3D-line skeleton in output from the final step of the *L-1 Medial Skeleton* implementation. The authors evidence how their algorithm could misses fine structures and incorrectly runs the skeleton in case of too sparse input point clouds [24]. To reach at least some skeleton's points alignment a lot of experiment have been done setting the propter parameters and getting in output the set $\boldsymbol{S}$ = $\{points \in Gorgonian\ point\ cloud\ skeleton\}$. Fortunately, the 3D skeleton as a 3D-line is necessary only for Method 1 in *Section 3.3.* This implies a preprocessing step to join the points in $\boldsymbol{S}$ and obtain the lines. For Methods 2 and 3, respectively in *Sections 3.4* and *3.5* the aligned points directly coming from *L-1 Medial Skeleton* are acceptable.

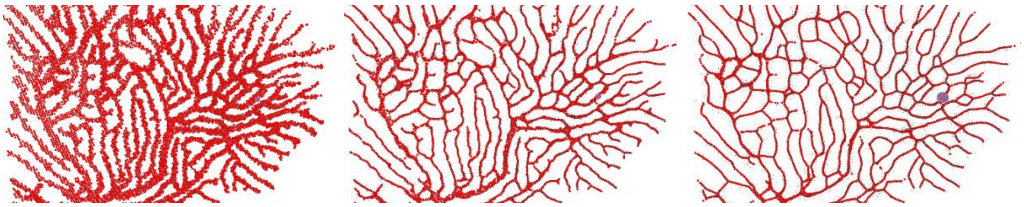

**Figure 6:** *Initial condition of the L-1 Medial Skeleton algorithm applied on a subset of* $\boldsymbol{P}$ *(left). After 10 iterations (center). After 10 more, the output subset of* $\boldsymbol{S}$ *(right). The blue sphere is a moving neighborhood.*

## 3.2 Layers thickness branches classification

The branches are automatically classified into 4 thickness layers using image morphological analysis on one of the original binary input images. The binarized image, coming from preprocessing steps, is elaborated iteratively by square pixel's neighbors through morphological operations as the opening: an erosion followed by a dilatation. Unconnected pixels have been removed and the layers are colorized by specific colors.

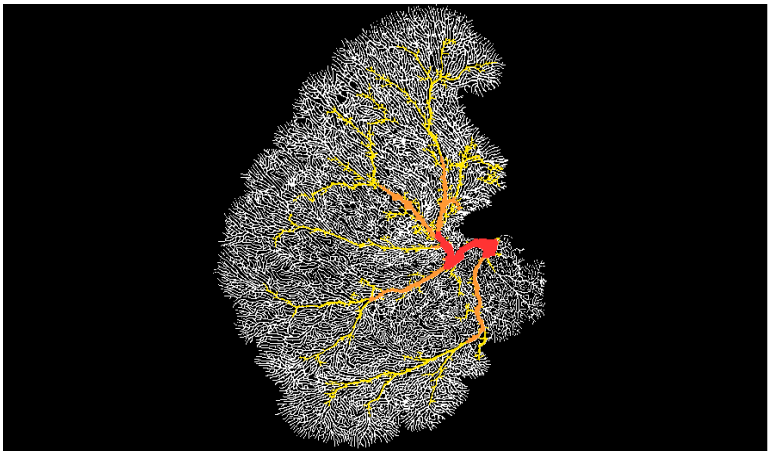

**Figure 7:** *Branched thickness classification on original binarized frame. One color for each thickness layer.*

## 3.3 Method 1: Manual & radius classes (M&RC)

As introduced before this method needs a 3D-line skeleton element. The points in the output set $\boldsymbol{S}$, coming from "*L-1 Medial Skeleton",* are manually connected by CAD software [28]. This step is extremely tedious and some human errors are introduced in the model during about the 12000 manual lines tracing. A second step regards the possibility to use a power CAD function, that, fixed the radius and selected the path, automatically generates a pipe/loft shape [29]. It is composed by pricewise cylinders/truncated cones merged each other. The above procedure has been done for each layer identified in *Section 3.2* (but it is not necessary to follow this specific classification as shown in *Fig.5*). The original point cloud $\boldsymbol{P}$ has been used as reference and the radius for each layer is set checking visually a 3D trial plot. The final mesh after simplification/smoothing process and geometrical errors removal is 30 Mb. About 120 man hours are needed.

## 3.4 Method 2: Semi-Automatic & radius classes (SA&RC)

For this method a simple but effective algorithm has been developed using as input four different point cloud sets obtained masking the original point cloud $\boldsymbol{P}$ using *Fig.7*. A masking tool in [5] allow to get $\boldsymbol{P_4}$ simply as $\boldsymbol{P}$, $\boldsymbol{P_3}$ as $\boldsymbol{P}$ minus the white layer branches, $\boldsymbol{P_2}$ as $\boldsymbol{P_3}$ minus the yellow layer branches and $\boldsymbol{P_1}$ as $\boldsymbol{P_2}$ minus the orange layer branches. The layer's radius is set visually using as reference $\boldsymbol{P}$ like in *Section 3.3*.

***1. For each point cloud set*** $\boldsymbol{P_{i=1\ldots4}}$
  ***1.1 Extract the point cloud skeleton set*** $\boldsymbol{S_i}$ ***using L-1 medial skeleton***
  ***1.2 Set the*** $\boldsymbol{r_i}$ ***=*** $\boldsymbol{layer_i}$ ***thickness***
  ***1.3 For each*** $\boldsymbol{point_J}$ $\boldsymbol{(x_J,y_J,z_J) \in S_i}$
    ***1.3.1 Mesh the sphere J with radius =*** $\boldsymbol{r_i}$ ***and center =*** $\boldsymbol{point_J}$
  ***End***
***End***
***2. Merge all the mesh*** $\boldsymbol{layer_i}$

The final mesh after simplification/smoothing process and geometrical errors removal is about 446 Mb. The computational running time of the algorithm is 2 hours.

## 3.5 Method 3: Semi-Automatic (SA)

This technique is the evolution of the previous one. It is more general and automated because leave-aside from the layer's classification radius. In this case the algorithm compute autonomously the specific radius for each point belonging to the skeleton point cloud $\boldsymbol{S}$ (*Section 3.1*), using as reference the original point cloud $\boldsymbol{P}$.

*1. Extract the point cloud skeleton set S using L-1 medial skeleton on P*
*2. For each point$_J$ ($x_J$,$y_J$,$z_J$) ∈ point cloud skeleton set S*
*2.1 Calculate the point density function*
*2.2 Evaluate the rules*
*2.3 Save the $r_J$*
*End*
*3. Improve the precedence r-vector modifying outlier radius (additional rules)*
*4. For each point$_J$ ($x_J$,$y_J$,$z_J$) ∈ point cloud skeleton set S*
*4.1 Mesh the sphere J with radius = $r_J$ and center = point$_J$*
*End*

The final mesh after simplification process and geometrical errors removal is 153 Mb. The computational running time is about 8 hours.

### 3.6 Method 4: Automated (A)

This is the only method that prescind from the 3D skeleton (*Section 3.1*). It works directly to the original point cloud $\boldsymbol{P}$ in a fully automatic approach. The algorithm meshes spheres for each point $\boldsymbol{J} \in \boldsymbol{S}$ using a fixed radius chosen by interactive way, depending on the density of the points into $\boldsymbol{P}$. The final mesh after simplification process and geometrical errors removal is about 370 Mb. The computational time is half an hour.

## 4 Results

A quantitative assessment process on above methods for complex point cloud meshing is presented and, taking as inspiration from [34], a top-down metric taxonomy is obtained.

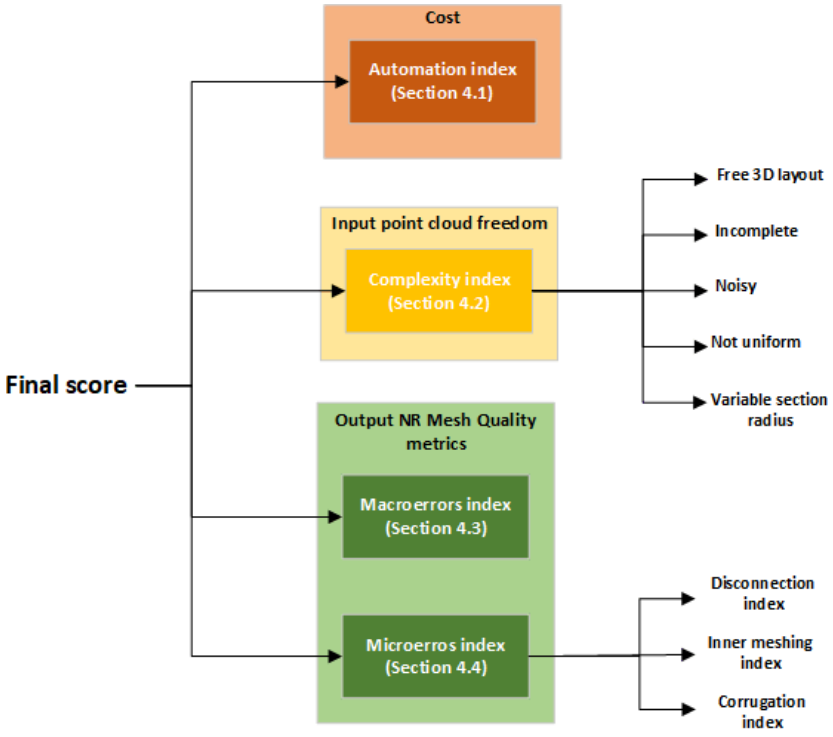


**Figure 8:** *Methods metrics taxonomy.*

For each method, cost, constraints on input point cloud and output mesh characteristics are evaluated for the final score. In *Sections 4.3* and *4.4*, related to mesh assessment, some NR metrics [32] are adopted from literature, some others have been defined by design from geometrical aspects. Regarding the constraints on the input point cloud, it is possible to summarize this concept by the degree of complexity (*Section 4.2*). A final metric related to cost parameter has been analyzed (*Section 4.1)*. The strength of this comprehensive procedure is the extreme simplicity that avoid black-box effect and give a quantitative and practical tool for the users that want to make a choice between different meshes methods, reducing the dimensionality of the problem into four main family of variables, put into a clear linear objective function.

$$\boldsymbol{Max}\ (A * Automation + B * Complexity - C * Macroerros - D * Micorerrors)$$

The values inlaid in the final objective function, are normalized by the maximum of its own family. Due the specific target, the multivariate family's coefficients can be set as more or less important by the human knowledge, using pairwise criteria comparison step as in the AHP method [35]. The results are summarized in *Table1.*

| Algorithms | Automation | Complexity | Macroerrors | Microerrors | Final score |
|---|---|---|---|---|---|
| Method 1 | 0% | 100% | 100% | 0% | **50** |
| Method 2 | 80% | 80% | 89% | 56% | **27** |
| Method 3 | 94% | 100% | 90% | 35% | **101** |
| Method 4 | 100% | 40% | 83% | 100% | **-73** |

**Table 1:** *The weights are set to A=1, B=1.5, C=1 and D=1.5 due the thesis goal stated in Section 1.2.*

## 4.1 Automation index

This index is crucial in order to manage problem with huge amount of data and it is directly related to the cost area. The index calculated for each method is:

$$Automation\ index = \frac{computational\ time}{computational\ time + manual\ time}$$

## 4.2 Complexity index

This index synthetizes input point cloud degrees of freedom that each method can deal with. An on-off evaluation has been done for each 5 complexity variables. The judgment is given considering each method peculiarity.

## 4.3 Macroerrors index (Dissimilarity index)

To quantify structural gaps between the models and the reality, every single one has been positioned in the same 2D view, as similar as possible to the original reference picture (*Fig. 7),* using a propter roto-translation matrix in a 3D visual environment [36]. After screen-shooting each of them, a locally adaptive threshold binarization was applied [7].

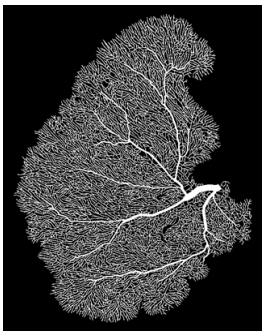

**Figure 9:** *Method 1.*

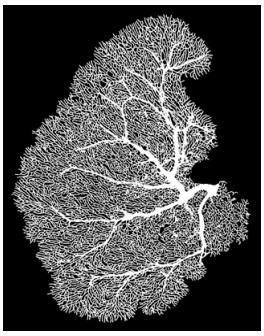

**Figure 10:** *Method 2.*

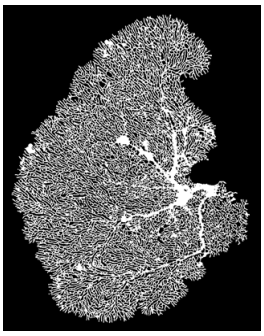

**Figure 11:** *Method 3.*

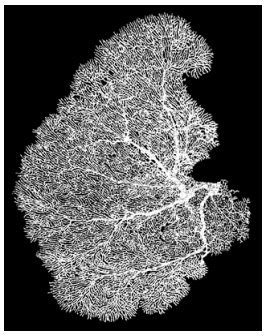

**Figure 12:** *Method 4.*

Then, based on feature-based registration algorithm, a rigid transformation to align binarized model's pictures to the reference picture has been applied, using the "*SSIM index"* to maximize the alignment [37], [31]. The index extracted from the pairs of registered images is the 1's complement of the 2D correlation applied the pixel matrixes.

## 4.4 Microerrors index

In this category there are several aspects that models approximate: separate pieces from the main structure, hidden surface modeling and surface pattern. Regarding this last aspect is clear how the spherical meshing causes a corrugated pattern (*Section 4.4.1*). Another issue related to the spherical meshing is the amount of inner meshing facets (*Section 4.4.2*) and the separate pieces from the object, due the lack of points density in that volume (*Section 4.4.3*).

### 4.4.1 Corrugation index

To quantify the amount of surface distortion caused by a modeling method instead of another, the concept used is similar the roughness [38]. The Method 1 has no corrugation due the manual CAD modeling. For each other three methods are calculated:

- ***Dist.m*** = distance between each sphere's center and the closer one, mediated on the number of spheres;
- ***mR*** = mean sphere's radius;
- ***Es*** = excursion of the max-min peak;
- ***Corrugation index*** = ***Es/mR*** .

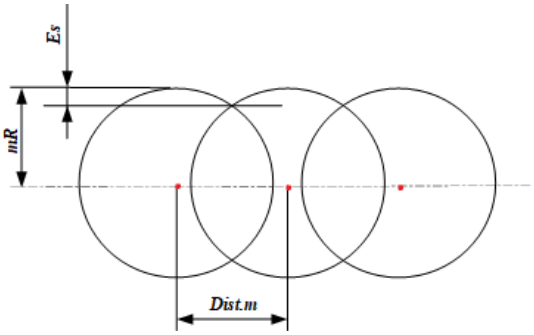


**Figure 13:** *2D graphical representation of* ***mR****,* ***Dist.m*** *and* ***Es.***

### 4.4.2 Disconnection index

To remove small isolated mesh fragments, a semi-automated approach on [36b] has been used. The % of non-connected component is calculated as:

$$Disconnection\ index = \frac{n\ isolated\ facets}{n\ total\ facets}$$

### 4.4.3 Inner meshing index

To quantify the proportion of inner meshing is used a simple but quite effective technique to compute the light occlusion value for each mesh vertex related to the difficulty to be enlightened [36b]. Therefore, is possible to select all the faces that have all their three vertices within occlusion range and compare this number to the total number of facets.

## 5 Conclusion

This work demonstrates the possibility to obtain remarkable results combining state-of-the-art concepts to a complex practical problem not yet been solved. It is a span of different methodology and points of view of the same issue that actual software's and algorithm's solution does not offer. After the final assessment step, is clear how for the thesis goals and relative weight setting, Method 3 seems to be the most interesting. Regarding practical problems as fluid-dynamic studies, modifying proper the weights in the objective function, Methods 1 and 2 should best fit with the specific goal. Anyway, the comparison between different approaches gives a full panoramic of the field of research and offers lot of food for thought that could trigger future works.

One of the most interesting question arising from this research, is the characterization of the rules that would produce a 2D manifold versus a fully 3D object. This is something planned to continue working on with the University of Hawaii, using the 3D model in output from the current work.

# 6 References


[5] Agisoft Metashape Professional Edition, version 1.5.

[7] Bradley, Derek and Roth, Gerhard, "*Adaptive Thresholding using the Integral Image*", J. Graphics Tools, volume 12, pages 13-21, 2007.

[8] Remondino Fabio, "*From point cloud to surface: the modeling and visualization problem*", International Archives of the Photogrammetry, Remote Sensing and Spatial Information Sciences, Vol. XXXIV-5/W10

[9] Yan-PingLin, Cheng-TaoWang, Ke-RongDai, "*Reverse engineering in CAD model reconstruction of customized artificial joint*", Medical Engineering & Physics, Volume 27, Issue 2, March 2005, Pages 189-193

[10] Ashok Kumar Patil, Pavitra Holi, Sang Keun Lee, Young Ho Chai, "*An adaptive approach for the reconstruction and modeling of as-built 3D pipelines from point clouds".* Automation in Construction 75:65-78 , March 2017

[11] J. Lee, C. Kim, H. Son, and C. Kim, "*Skeleton-based 3D reconstruction of as-built pipelines from laser-scan data*", Automation in Construction**,** Volume 35, November 2013, Pages 199-207

[12] K.Kawashima, S.Kanai, H.Date, "*Automatic recognition of a piping system from large-scale terrestrial laser scan data*", International Archives of the Photogrammetry, Remote Sensing and Spatial Information Sciences, Volume XXXVIII-5/W12, 2011.

[13] François Goulette, "*Automatic CAD Modeling of Industrial Pipes from Range Images*", 3-D Digital Imaging and Modeling, 1997.

[14] Deyu Sun, Maryam E. Rettmann, David R. Holmes, III, Cristian Linte, Bruce Cameron, Jiquan Liu, Douglas Packer and Richard A. Robb, "*Anatomic Surface Reconstruction from Sampled Point Cloud Data and Prior Models*", Stud Health Technol Inform. 2014; 196: 387–393.

[15] Pingbo Tang, Daniel Huber, Burcu Akinci, Robert Lipman, Alan Lytle, "*Automatic reconstruction of as-built building information models from laser-scanned point clouds: A review of related techniques*", Automation in Construction 19(7):829-843, November 2010

[16] Angela Budroni, Jan Boehm "*Automated 3D Reconstruction of Interiors from Point Clouds*", International Journal of Architectural Computing 8(1):55-73, January 2010.

[17] Gabriele Guidi, Michele Russo, Davide Angheleddu, "*3D survey and virtual reconstruction of archeological sites*", Digital Applications in Archaeology and Cultural Heritage 1(2), 2014.

[18] Kotaro Yamafune, "*Using Computer Vision Photogrammetry (Agisoft PhotoScan) to Record and Analyze Underwater Shipwreck Sites*", Thesis for: Doctor of Philosophy, Advisor: Filipe Castro, May 2016.

[19] Dong-Ming Yan, Julien Wintz, Bernard Mourrain, Wenping Wang, Frédéric Boudon, et al., "*Efficient and robust reconstruction of botanical branching structure from laser scanned points.",* CAD/Graphics 2009, Aug 2009, Yellow Mountain City, China. pp.572-575. ffinria-00436480f

[20] Nina Amenta, Choi and Kolluri, "*The power crust."* 6th ACM Symposium on Solid Modeling, 2001, pages 249-260

[21] Young-Hoon Jin and Won-Hyung Lee, "*Fast Cylinder Shape Matching Using Random Sample Consensus in Large Scale Point Cloud."* Applied Sciences 2019, 9, 974.

[22] M. Zwicker and C. Gotsman, "*Meshing Point Clouds Using Spherical Parameterization*", Eurographics Symposium on Point-Based Graphics, 2004

[23] Hong-Wei Lin, Chiew-Lan Tai, Guo-Jin Wang, "*A mesh reconstruction algorithm driven by an intrinsic property of a point cloud*", Computer-Aided Design 36 1–9, 2004

[24] Hui Huang, Shihao Wu, Daniel Cohen-Or, Minglun Gong, Hao Zhang, Guiqing Li, Baoquan Chen, "*L-1 medial skeleton of point cloud*." ACM Transactions on Graphics , volume 32, number 4, pages 65:1--65:8, 2013. L-1 medial skeleton software

[25] Andrea Tagliasacchi, Hao Zhang, Daniel Cohen-Or, "*Curve Skeleton Extraction from Incomplete Point Cloud."* ACM Transactions on Graphics 28(3) , 2009

[26] Junjie Cao, Andrea Tagliasacchi, Matt Olson, Hao Zhang, Zhixun Su, "Point Cloud Skeletons via Laplacian-Based Contraction." IEEE international conference on shape modeling and applications (smi), 2010

[27] Sheng Wu, Weiliang Wen, Boxiang Xiao, Xinyu Guo, Jianjun Du, Chuanyu Wang and Yongjian Wang, "An Accurate Skeleton Extraction Approach From 3D Point Clouds of Maize Plants." Frontiers in Plant Science 10:248 , 2019

[28] Inventor, Autodesk

[29] SolidWorks, Dassault Systèmes

[31] Guillaume Lavoué, Rafal Mantiuk "*Quality Assessment in Computer Graphics."* Visual Signal Quality Assessment – Quality of Experience (QoE), Springer, pp.243-286, Chaper 2, 2015, 978-3-319-10368-6.

[32] Chetouani and Aladine, "*A 3D Mesh Quality Metric based on Features Fusion",* Electronic Imaging, pages 4-8, 2017

[34] Oussama Ennafii, Arnaud Le Bris, Florent Lafarge, Clément Mallet, "A learning approach to evaluate the quality of 3D city models.", Photogrammetric engineering and remote sensing, Asprs American Society for Photogrammetry, 2019

[35] Thomas L. Saaty, "*Multicriteria decision making - the analytic hierarchy process".* Planning, priority setting, resource allocation, RWS Publishing, Pittsburgh, 1988.

[36a] P. Cignoni, M. Callieri, M. Corsini, M. Dellepiane, F. Ganovelli, G. Ranzuglia, *"MeshLab: An Open-Source Mesh Processing Tool"*, Sixth Eurographics Italian Chapter Conference, page 129-136, 2008.

[36b] MeshLab software

[37] *Zhou, W., A. C. Bovik, H. R. Sheikh, and E. P. Simoncelli. "Image Qualifty Assessment: From Error Visibility to Structural Similarity."* IEEE Transactions on Image Processing. Vol. 13, Issue 4, April 2004, pp. 600–612.

[38] Whitehouse, David, "*Surfaces and their Measurement*" Boston: Butterworth-Heinemann, ISBN 978-0080972015.